Journal Name

COMMUNICATION

Oligoalanine Helical Callipers for Cell Penetration

Marta Pazo,[a] Marisa Juanes,[a] Irene Lostalé-Seijo[a] & Javier Montenegro[a]*

Received 00th January 20xx,

Accepted 00th January 20xx

DOI: 10.1039/x0xx00000x

www.rsc.org/

Even for short peptides that are enriched in basic amino acids, the large chemical space that can be spanned by combinations of natural amino acids hinders the rational design of cell penetrating peptides. We here report on short oligoalanine scaffolds for the fine-tuning of peptide helicity in different media and the study of cell penetrating properties. This strategy allowed the extraction of the structure/activity features required for maximal membrane interaction and cellular penetration at minimal toxicity. These results confirmed oligoalanine helical callipers as optimal scaffolds for the rational design and the identification of cell penetrating peptides.

Positively charged molecules and macromolecules with a certain degree of hydrophobicity can interact with anionic membranes and be taken up by cells.[1-9] Initial evidences of these penetrating capacities were found in certain sequences of proteins enriched in basic amino acids.[1,2] The subsequent development led to the emergence of the cell penetrating peptides (CPPs).[10,11] In the taxonomy of penetrating peptides, the oligoarginines and analogous sequences have been assigned to the cationic/hydrophilic and non-structured class of peptides.[10,11] However, although pure hydrophobic penetrating peptides have also been reported,[12,13] oligoarginines certainly possess intrinsic amphiphilicity as each arginine contains three methylene units per guanidium group.[1] Additionally, the peptide cargo or the fluorophore tracking moiety may add extra hydrophobicity to the peptide and have direct implications in the internalization.[2,14] The peptide plasticity and the conformational switch from random coil to amphiphilic structures have been identified as important descriptors in several efficient natural and artificial CPPs.[15-19] Intriguing reports have established the importance of the spatial distribution and orientation of the cationic and the hydrophobic residues to achieve an efficient cell membrane translocation.[13,20-23] In this regard, the alpha helical motif has been widely applied by chemists and biochemists to generate and study cationic-amphiphilic penetrating structures.[2,15,16,18,19,24-29] Artificial helical foldamers, polymers and supramolecular structures have also been designed and confirmed as cell penetrating scaffolds.[2,30-36] However, despite the large progress achieved during the last years, CPPs still remain a source of controversy in terms of structure/activity relationships, mechanism of cell entry and prediction of penetrating properties.[1,10,37,38] Therefore, methodologies for the rational design of penetrating peptide sequences are essential tools for the discovery of the next generation of CPPs with increased efficiency and reduced toxicity. Some elegant strategies building on peptide cyclization, structural fixation and hydrophobicity accumulation have been recently studied to rationalize the penetrating capabilities of CPPs.[21,37,39,40] However, even for short sequences containing a high fraction of basic and hydrophobic amino acids, the enormous chemical space that can be spanned by permutations of the proteinogenic natural amino acids constitutes a critical limitation for the extraction of insightful conclusions about the activity of penetrating peptides. Among all the natural amino acids, alanine has the strongest alpha-helical stabilizing character (– 0.77 kcal/mol).[24,41] Although no helicity was reported, the strong helical propensity of alanine has been exploited in inspiring short penetrating peptides.[24] Herein we report on oligoalanines scaffolds as helical callipers to study the consequences in cell uptake and cytoxicity of the helical folding in different environments (buffer and liposomes). This simple model allowed us to identify a peptide hit bearing only three arginines and three leucines residues and with a strong membrane affinity, cell internalization capacity and low toxicity at the working conditions.

The oligoalanine peptides of this study (**P_1-P_8**, Fig 1) were synthesized by solid phase peptide synthesis and they were terminated with a 5-carboxytetramethylrhodamine fluorophore (TAMRA) (see supporting information, Fig. S1). The total sequence was composed of 16 amino acids that were sufficient to stabilize two heptad helical turns (Fig. 1A). Peptide folding was characterized by circular dichroism in aqueous buffer (HKR, pH = 7.4), liposomes (EYPC) and trifluoroethanol (Fig. 1B and Fig. S2). In these oligoalanine templates, we incorporated a fixed number of three cationic arginines and a

[a] *Centro Singular de Investigación en Química Biolóxica e Materiais Moleculares (CIQUS), Departamento de Química Orgánica, Universidade de Santiago de Compostela, 15782 Santiago de Compostela, Spain. *e-mail: javier.montenegro@usc.es*

Electronic Supplementary Information (ESI) available: [details of any supplementary information available should be included here]. See DOI: 10.1039/x0xx00000x.

A)

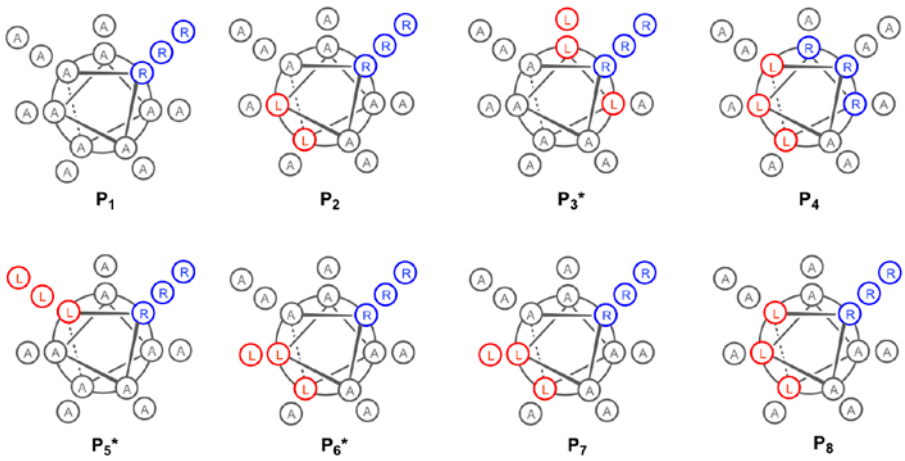

B)

Peptide	% Helicity at 40 °C		
	Liposomes	*HKR*	*TFE*
P_1	0.2	9.7	40.7
P_2	6.5	12.4	42.8
P_3	12.7	21.7	45.8
P_4	13.3	1.9	42.3
P_5	29.5	19.3	57.8
P_6	29.9	35.1	77.0
P_7	31.6	16.1	54.8
P_8	49.2	12.8	55.7

Fig. 1. A) Heptad-based wheel diagram for the helical conformation of **P_1-P_8**. The N-terminus of all peptides was coupled to a TAMRA (5-carboxytetramethylrhodamine) fluorophore. Note that **P_3**, **P_5** and **P_6** (labelled with an asterisk) have a hexanoic linker between the peptide N-Terminal and the TAMRA (see supporting information). B) Table showing the % of helicity of the eight peptides (**P_1-P_8**) at 40 °C in HKR buffer, egg yolk phosphatidylcholine (EYPC) liposomes and trifluoroethanol (TFE).

number of three, two or none hydrophobic leucines. Pure alanine/arginine combinations yielded peptides with a very poor helical behaviour and negligible uptake in HeLa cells (**P_1**, Fig. S3). The incorporation of two leucine hydrophobic amino acids improved helicity in liposomes (**P_1** and **P_2**), although peptide uptake was insignificant compared with octaarginine (Fig. 2A). A third leucine triggered a higher increase in peptide helicity and cellular uptake (Fig. 1B and Fig. 2A). Alignment of the three-guanidinium side chains was beneficial for helicity of the oligoalanine scaffold in the membrane as can be observed by comparing **P_4** and **P_8** (13% *vs* 50% helicity in liposomes, Fig. 1). The presence of a hexanoic linker between the peptide and the fluorophore slightly increased helicity in buffer and reduced it in liposomes (see **P_6** *vs* **P_7** in Fig. 1 and supporting information). The proximity of the hydrophobic leucines to the aligned arginines stabilized the helicity of the peptide in buffer (**P_3** and **P_5**). On the other hand, for the peptides with three aligned arginines, the radial distribution of the three leucines increased peptide helicity and maximized the difference of helical behaviour from buffer to liposomes (Fig. 1, compare **P_7** *vs* **P_8**). This maximized helical difference can be rationalized by a potential carpet-like peptide disposition that would accommodate the guanidinium residues towards the aqueous buffer and maximize leucine hydrophobic interactions with the hydrophobic part of the bilayer. The final selection of TAMRA-labelled peptides covered a wide helical range in lipid membranes from random coil (**P_1**) to 50% of helicity (**P_8**).

With this collection of peptides we carried out uptake experiments by incubating HeLa cells with the peptides at different concentrations (0.5 to 10 µM). After incubation, cells were thoroughly washed with buffer and trypsinized to remove all membrane bound peptides and the uptake was quantified by flow cytometry (Fig. 2A, see supporting information). The dose response cytometry showed a low level of cellular uptake for the peptides with less than 30% helicity in liposomes (**P_1**, **P_2**, **P_3** and **P_4**, Fig. 2B). Peptides **P_5** and **P_6**, with certain helical behaviour in liposomes (~ 30%) but also in buffer (20% and 35% respectively), exhibited a slightly higher level of uptake, which was still far below the octaarginine control (Fig. 2A). However, peptides **P_7** and **P_8** with the highest helicity in liposomes (32% and 50% respectively) and the maximum helicity difference in the transition from buffer to liposomes, presented a much higher cellular internalization similar to the prototypical octaarginine peptide (**R_8**). This enhanced uptake was more than five times higher than that achieved for **P_5** and **P_6**, which showed an intermediate and stable (~ 25%) helicity in buffer and lipids (Fig. 1, Fig. 2A).

Cytotoxicity studies were next carried out by the MTT colorimetric assay, which reports on cell mitochondrial metabolic activity (Fig. 2C, see supporting information). Intriguingly, these studies revealed that peptide uptake was not proportional to toxicity. Representation of cell viability for the different peptides revealed that the more toxic peptides at 5 µM were the peptides with a higher helical content in the buffer media **P_3** and **P_6** (Fig. 2C). These two more toxic peptides (**P_3** and **P_6**) were more helical in buffer compared to liposomes (Fig. 1B). In contrast, the peptides presenting the opposite switch in helicity, from low in buffer to high in lipids (**P_5**, **P_7** and **P_8**), showed good cell viabilities independently of their stronger uptake in cells (Fig. 2B and 2C). Epifluorescence micrographs of the cells incubated with the peptide collection were in good agreement with the cytometry results and showed a punctate fluorescence pattern (Fig. S3 and Fig. S4). We next carried out internalization studies at low temperature and in the presence of endocytic inhibitors for the best hit (**P_8**) (Fig. S6). The full inhibition of the uptake of **P_8** observed at low temperature 4 °C confirmed that the peptide internalization was energy dependent.

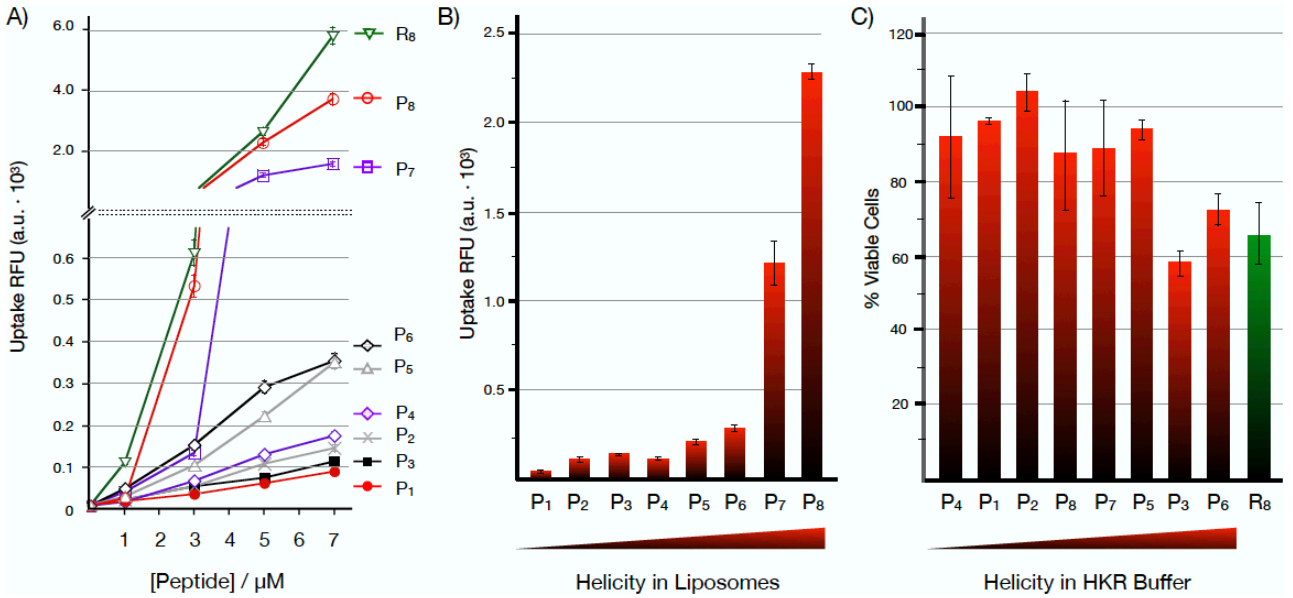

Fig. 2. Cellular uptake and viability of oligoalanine callipers. A) Cytometry uptake quantification. Cells were incubated with the peptides (30 min) at the different concentrations in HKR buffer and trypsinized prior cytometer fluorescence quantification. The ordinate axis has been cut to allow comparison. The TAMRA labelled octaarginine peptide (**R_8**) is shown in green. B) Raw fluorescence intensity for the uptake of the different peptides at 5 μM. In the abscise axis the peptides are ordered by increasing helicity in liposomes. C) Cell viability (MTT) of the different peptides at 5 μM. In the abscise axis the peptides are ordered by increasing helicity in HKR buffer (pH = 7.4). The cytoxicity of **R_8** at 5 μM is shown in green.

We could observe that Dynasore, an inhibitor of dynamin dependent endocytosis, fully blocked peptide uptake. Cell membrane cholesterol depletion by methyl-β-cyclodextrin strongly reduced the fluorescence signal, which indicated that caveolin-mediated endocytosis was the major pathway for **P_8** internalization (Fig. S6). This is in agreement with previous results observed for helical poly-prolines.[3] We finally investigated and compared the cell penetration properties of **P_8** in three different cell lines (HeLa, A549 and SF9) by cytometry and spinning-disk confocal fluorescent microscopy (Fig. 3 and Fig. S7). The confocal 3D projections in the different cells showed the corresponding punctate fluorescence patterns in HeLa and A549 cells (Fig. 3), that colocalized with lysosomes at longer incubation times (Fig. S5), confirming that the peptide remained trapped in endosomes. However, the 3D confocal micrographs of **P_8** in SF9 cells presented a diffuse cytosolic distribution, which confirmed that the entry mechanism and the final internal distribution of this peptide could be cell dependent. Finally, we studied the stability and uptake of **P_8** in the presence of serum (Fig. S11). Serum reduced only slightly the uptake of this peptide in HeLa and A549 cells (Fig. S11A). The half-life of this peptide in serum is ~ 2.2 h, similar to that described for R9.

In summary, we introduce oligoalanines as suitable scaffolds for the precise control of the helical behaviour of penetrating peptides. This strategy allowed us to identify peptides with a strong cell penetrating capacity bearing only three arginine and three leucine amino acids. Circular dichroism studies indicated that arginine alignment and leucine radial distribution was the optimal amino acid disposition to increase the helicity in the transition from the aqueous buffer to the lipid environment. For the peptide collection reported here, this helical transition improved cell uptake while it did not increase peptide toxicity. In contrast, amphiphilic oligoalanines with stable helical behaviour in buffer were not efficiently taken up by cells and were more toxic. The best hit of the series (**P_8**) showed the maximum helical character in liposomes and the highest difference in helicity from water to liposomes. **P_8** was mainly internalized by caveolin-mediated endocytosis and, not surprisingly, the internalization was dependent on the cell line. The results reported here validated oligoalanines scaffolds as helical callipers for the study of rationally designed peptides with cell penetrating capabilities.

Acknowledgements

This work was partially supported by the Spanish Agencia Estatal de Investigación (AEI) [CTQ2014-59646-R, SAF2017-89890-R], the Xunta de Galicia (ED431G/09, ED431C 2017/25 and 2016-AD031) and the ERDF. M. P. thanks the Xunta de Galicia for a pre-doctoral fellowship (ED481A-2017/142), and M.J. MINECO for a F.P.I. fellowship. J.M. received a Ramón y Cajal (RYC-2013-13784), an ERC Starting Investigator Grant (DYNAP-677786) and a Young Investigator Grant from the Human Frontier Science Research Program (RGY0066/2017).

References

1 P. M. Fischer, *Med. Res. Rev.*, 2007, **27**, 755–795.
2 D. Kalafatovic and E. Giralt, *Molecules*, 2017, **22**, 1929–1967.
3 S. Pujals and E. Giralt, *Adv. Drug. Deliv. Rev.*, 2008, **60**, 473–484.

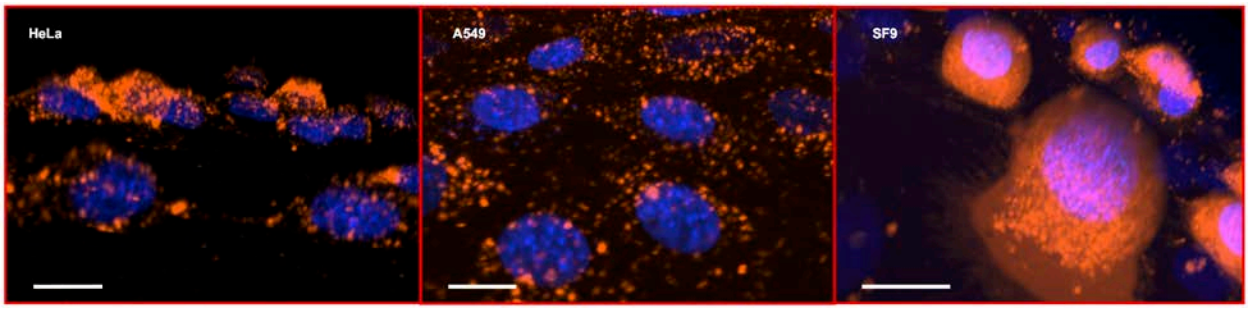

Fig. 3. Spinning-Disk Confocal 3D projections of $\mathbf{P_8}$ in different cells (HeLa, A549 and SF9). Peptide was incubated with cells at 5 µM (30 min, HKR buffer). Cells were washed with HKR buffer three times and observed by microscopy. Scale bars are 20 µm. The 3D projection was obtained from the different individual confocal planes with Imaris bitplane © 9.0.0 software.

4 Ü. Langel, *Cell-penetrating peptides: methods and protocols.*, 2011. Springer-Verlag GmbH: New York.
5 C. Palm-Apergi, P. Lönn and S. F. Dowdy, *Mol. Ther.*, 2012, **20**, 695–697.
6 E. G. Stanzl, B. M. Trantow, J. R. Vargas and P. A. Wender, *Acc. Chem. Res.*, 2013, **46**, 2944–2954.
7 G. Gasparini, E.-K. Bang, J. Montenegro and S. Matile, *Chem. Commun.*, 2015, **51**, 10389–10402.
8 M.-A. Sani and F. Separovic, *Acc. Chem. Res.*, 2016, **49**, 1130–1138.
9 A. Fuertes, J. Marisa, J. R. Granja and J. Montenegro, *Chem. Commun.*, 2017, **53**, 7861–7871.
10 W. B. Kauffman, T. Fuselier, J. He and W. C. Wimley, *Trends Biochem. Sci.*, 2015, **40**, 749–764.
11 L. Brambilla and D. Rossi, *Trends Pharm. Sci.*, 2017, **38**, 406–424.
12 B. M. deRonde, N. D. Posey, R. Otter, L. M. Caffrey, L. M. Minter and G. N. Tew, *Biomacromolecules*, 2016, **17**, 1969–1977.
13 D. Bhunia, P. Mondal, G. Das, A. Saha, P. Sengupta, J. Jana, S. Mohapatra, S. Chatterjee and S. Ghosh, *J. Am. Chem. Soc.*, 2018, **140**, 1697–1714.
14 A. Erazo-Oliveras, K. Najjar, L. Dayani, T.-Y. Wang, G. A. Johnson and J.-P. Pellois, *Nat. Meth.*, 2014, **11**, 861–867.
15 M. Magzoub, L. E. G. Eriksson and A. Gräslund, *Biochim. Biophys. Acta*, 2002, **1563**, 53–63.
16 W. Li, F. Nicol and F. C. Szoka, *Adv. Drug. Deliv. Rev.*, 2004, **56**, 967–985.
17 S. Deshayes, K. Konate, G. Aldrian, L. Crombez, F. Heitz and G. Divita, *Biochim. Biophys. Acta*, 2010, **1798**, 2304–2314.
18 G. Wiedman, S. Y. Kim, E. Zapata-Mercado, W. C. Wimley and K. Hristova, *J. Am. Chem. Soc.*, 2017, **139**, 937–945.
19 M. Akishiba, T. Takeuchi, Y. Kawaguchi, K. Sakamoto, H.-H. Yu, I. Nakase, T. Takatani-Nakase, F. Madani, A. Gräslund and S. Futaki, *Nat. Chem.*, 2017, **9**, 751–761.
20 D. S. Daniels and A. Schepartz, *J. Am. Chem. Soc.*, 2007, **129**, 14578–14579.
21 G. Lättig-Tünnemann, M. Prinz, D. Hoffmann, J. Behlke, C. Palm-Apergi, I. Morano, H. D. Herce and M. C. Cardoso, *Nat. Commun.*, 2011, 2:453.
22 J. S. Appelbaum, J. R. La Rochelle, B. A. Smith, D. M. Balkin, J. M. Holub and A. Schepartz, *Chem. Biol.*, 2012, **19**, 819–830.
23 Y. A. Nagel, P. S. Raschle and H. Wennemers, *Angew. Chem.*, 2017, **56**, 122–126.
24 A. Ho, S. R. Schwarze, S. J. Mermelstein, G. Waksman and S. F. Dowdy, *Cancer Res.*, 2001, **61**, 474–477.
25 H. Tang, L. Yin, K. H. Kim and J. Cheng, *Chem. Sci.*, 2013, **4**, 3839–3844.
26 Y. Bai, L. Nguyen, Z. Song, S. Peng, J. Lee, N. Zheng, I. Kapoor, L. D. Hagler, K. Cai, J. Cheng, H. Y. E. Chan and S. C. Zimmerman, *J. Am. Chem. Soc.*, 2016, **138**, 9498–9507.
27 S. R. Perry, T. A. Hill, A. D. de Araujo, H. N. Hoang and D. P. Fairlie, *Org. Biomol. Chem.*, 2018, **16**, 367–371.
28 I. Louzao, R. García-Fandiño and J. Montenegro, *J. Mat. Chem. B*, 2017, **5**, 4426–4434.
29 I. Lostalé-Seijo, I. Louzao, M. Juanes and J. Montenegro, *Chem. Sci.*, 2017, **8**, 7923-7931.
30 E. R. Gillies, F. Deiss, C. Staedel, J.-M. Schmitter and I. Huc, *Angew. Chem. Int. Ed.*, 2007, **46**, 4081–4084.
31 A. D. Bautista, C. J. Craig, E. A. Harker and A. Schepartz, *Curr. Opin. Chem. Biol.*, 2007, **11**, 685–692.
32 M. Okuyama, H. Laman, S. R. Kingsbury, C. Visintin, E. Leo, K. L. Eward, K. Stoeber, C. Boshoff, G. H. Williams and D. L. Selwood, *Nat. Meth.*, 2007, **4**, 153–159.
33 K. Petkau-Milroy, M. H. Sonntag, A. H. A. M. van Onzen and L. Brunsveld, *J. Am. Chem. Soc.*, 2012, **134**, 8086–8089.
34 J. W. Checco, E. F. Lee, M. Evangelista, N. J. Sleebs, K. Rogers, A. Pettikiriarachchi, N. J. Kershaw, G. A. Eddinger, D. G. Belair, J. L. Wilson, C. H. Eller, R. T. Raines, W. L. Murphy, B. J. Smith, S. H. Gellman and W. D. Fairlie, *J. Am. Chem. Soc.*, 2015, **137**, 11365–11375.
35 C. Gehin, J. Montenegro, E.-K. Bang, A. Cajaraville, S. Takayama, H. Hirose, S. Futaki, S. Matile and H. Riezman, *J. Am. Chem. Soc.*, 2013, **135**, 9295–9298.
36 J. M. Priegue, D. N. Crisan, J. Martínez-Costas, J. R. Granja, F. Fernandez-Trillo and J. Montenegro, *Angew. Chem. Int. Ed.*, 2016, **55**, 7492–7495.
37 M. Hansen, K. Kilk and Ü. Langel, *Adv. Drug. Deliv. Rev.*, 2008, **60**, 572–579.
38 M. Hällbrink, K. Kilk, A. Elmquist, P. Lundberg, M. Lindgren, Y. Jiang, M. Pooga, U. Soomets and Ü. Langel, *Int. J. Pept. Res. Ther.*, 2005, **11**, 249–259.
39 S. Mondal, M. Varenik, D. N. Bloch, Y. Atsmon-Raz, G. Jacoby, L. Adler-Abramovich, L. J. W. Shimon, R. Beck, O. Regev, Y. Miller and E. Gazit, *Nat. Commun.*, 2017, **8**, 8:14018.
40 S. Schmidt, M. J. W. Adjobo-Hermans, R. Kohze, T. Enderle, R. Brock and F. Milletti, *Bioconjugate Chem.*, 2017, **28**, 382–389.
41 S. Marqusee, V. H. Robbins and R. L. Baldwin, *Proc. Natl. Acad. Sci. U. S. A.*, 1989, **86**, 5286–5290.